

A Bow-Shock Nebula Around a Compact X-ray Source in the Supernova Remnant IC 443

Charles M. Olbert¹, Christopher R. Clearfield¹, Nikolas E. Williams¹, Jonathan W. Keohane¹,
Dale A. Frail²

Accepted to the Astrophysical Journal Letters as of March 15th, 2001.

ABSTRACT

We present spectra and high resolution images of the hard X-ray feature along the southern edge of the supernova remnant IC 443. Data from the *Chandra X-ray Observatory* reveal a comet-shaped nebula of hard emission, which contains a softer point source at its apex. We also present $\lambda 20$ cm, $\lambda 6$ cm, and $\lambda 3.5$ cm images from the *Very Large Array* that clearly show the cometary nebula. Based on the radio and X-ray morphology and spectrum, and the radio polarization properties, we argue that this object is a synchrotron nebula powered by the compact source that is physically associated with IC 443. The spectrum of the soft point source is adequately but not uniquely fit by a black body model ($kT=0.71\pm 0.08$ keV, $L=(6.5\pm 0.9)\times 10^{31}$ ergs⁻¹). The cometary morphology of the nebula is the result of the supersonic motion of the neutron star ($V_{NS}\simeq 250\pm 50$ km s⁻¹), which causes the relativistic wind of the pulsar to terminate in a bow shock and trail behind as a synchrotron tail. This velocity is consistent with an age of 30,000 years for the SNR and its associated neutron star.

Subject headings: ISM: supernova remnants — ISM: individual object: IC 443 — stars: neutron
— stars: pulsars: individual object: CXOU J061705.3+222127

1. Introduction

The mixed-morphology Galactic supernova remnant IC 443 (l,b = 189.1°, +3.0°) has been the subject of extensive studies at all wavelength bands (Fesen 1984; Braun & Strom 1986; van Dishoeck, Jansen & Phillips 1993; Asaoka & Aschenbach 1994). IC 443 is especially well known for its clear interaction with surrounding molecular clouds (Burton *et al.* 1990; Bocchino & Bykov(2000)). With its large variety of shocked molecular species detected along its SE edge, IC 443 has become a standard laboratory for studying shock chemistry (van Dishoeck *et al.* 1993 and references therein).

IC 443 is also of interest because it is coincident with the unidentified EGRET source 2EG J0618+2234 (Sturmer & Dermer 1995; Esposito *et al.* 1996), and thus has stimulated a good deal of theoretical work aiming to explain the production of GeV γ -rays by shell SNRs (Sturmer, Dermer & Mattox 1996; Sturmer *et al.* 1997; Gaisser, Protheroe & Stanev 1998; Baring *et al.* 1999; Bykov *et al.* 2000).

In the X-ray band, Petre *et al.* (1988) found that the bulk of the emission was thermal in origin with a temperature $\sim 10^7$ K, typical of middle-aged SNRs. However, Wang *et al.* (1992) found evidence in

¹North Carolina School of Science and Mathematics, 1219 Broad St., Durham, NC 27705

²National Radio Astronomy Observatory, P. O. Box O, Socorro, NM 87801

the *Ginga* satellite data for a hard X-ray component in the spectrum of IC 443 extending up to 20 keV. Follow-up observations with the *ASCA* satellite revealed that the bulk of this hard X-ray emission came from a single, unresolved feature located along the edge of the radio shell where the SNR/molecular cloud interaction was strongest (Keohane *et al.* 1997, hereafter K97). Furthermore, the hard X-ray feature is positionally coincident with a region where the radio spectral index is considerably flatter than the SNR as a whole (i.e. $\alpha < 0.24$ vs $\alpha = 0.42$, where $F_\nu \propto \nu^{-\alpha}$) (Green 1986; Kovalenko, Pynzar & Udal'Tsov 1994).

K97 considered different explanations for the origin of this hard X-ray emission, and favored a model in which synchrotron emission was being produced by TeV electrons in a region of enhanced particle acceleration, resulting from the SNR/molecular cloud interaction. Recent BeppoSAX data analyzed by Bocchino & Bykov (2000) also support the K97 interaction model. An equally viable model, favored by Chevalier (1999, hereafter C99), posits that the hard X-ray feature is synchrotron emission powered by an energetic neutron star. To distinguish between these two competing hypotheses we have undertaken high resolution X-ray and radio observations toward the hard X-ray feature. These new Chandra and VLA observations strongly favor C99's neutron star hypothesis.

2. Observations and Analysis

2.1. Chandra X-Ray Observatory

The *Chandra X-Ray Observatory* performed a short (10 ks) observation of IC 443 on April 10, 2000 during the first cycle of guest observations (A01). The hard X-ray feature was centered on the I3 chip of the Advanced CCD Imaging Spectrometer (ACIS). To produce Chandra event files, we followed the standard CIAO procedures outlined in Version 1.3 of the *CIAO* Beginner's Guide for *CIAO* Release 1.1, using the `acisD2000-01gainN0001.fits` gain file. From the events file, we extracted high resolution images in both hard ($E > 2.1$ keV) and soft ($E < 2.1$ keV) spectral bands. Smoothed versions of these images are presented in Figure 1.

The hard X-ray source is resolved by this high resolution ($\sim 1''$) Chandra observation (Figure 1) as a nebular region of diffuse emission with a cometary tail. Within the nebula there is an unresolved point source that we have designated as *CXOU J061705.3+222127*. The nebula of hard emission exhibits bow-shock morphology with a width of $\simeq 35''$ and a minimum standoff distance of $r_s \simeq 8.5''$. The X-ray point source lies at the apex of the nebula, located at (epoch 2000) $\alpha = 06^h 17^m 05.31^s$, $\delta = 22^\circ 21' 27''.3$, with errors of $\pm 2''$ in each coordinate. It is especially visible in the soft ($E < 2.1$ keV) X-ray band (Figure 1).

Likewise, in order to compare the X-ray luminosity of the cometary nebula with statistical studies of pulsar wind nebulae (PWNe) (e.g. Seward & Wang 1988, see §3), we integrated the power-law model of K97 over the *Einstein* band (0.2-4 keV) – thus deriving $L_x \sim 5 \times 10^{33} d^2 (1.5 \text{ kpc})^{-2} \text{ erg s}^{-1}$. Inherent in this L_x calculation is the assumption that the cometary nebula is dominated in soft X-rays by the same power-law exhibited at hard energies with *ASCA*. The Chandra flux (over the same range) yields consistent results, albeit with larger uncertainties.

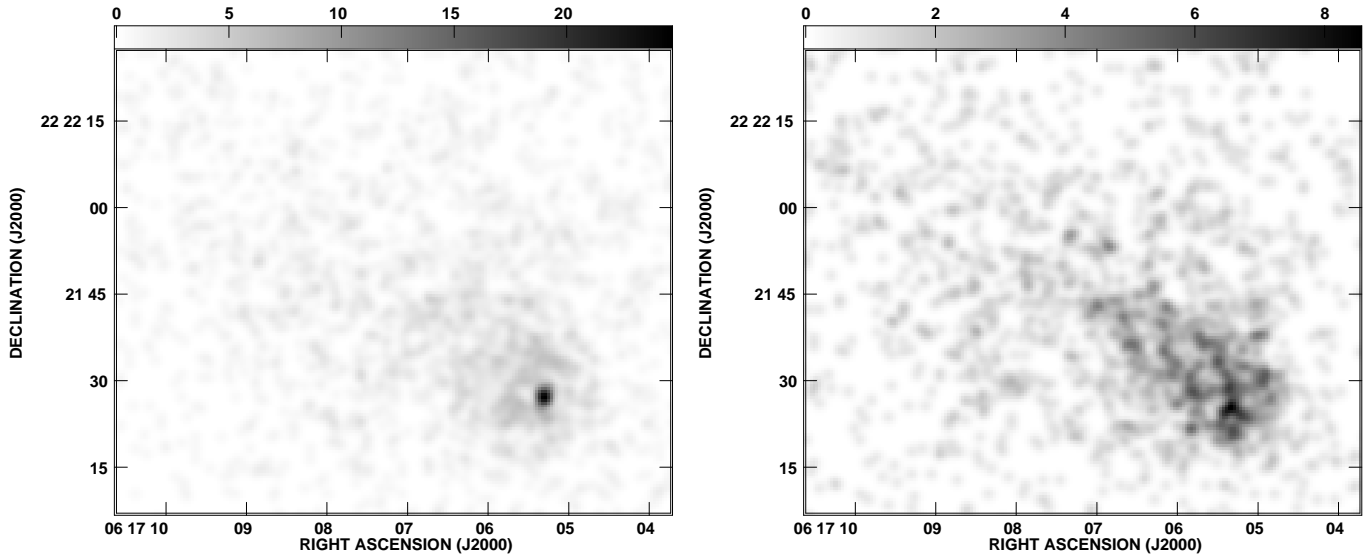


Fig. 1.— X-ray intensity images of the hard X-ray feature on the southern edge of IC 443. The image on the left is in the soft ($E < 2.1$ keV) photon energy band, scaled between 0 to 24.6 counts per beam. The image on the right is in the hard ($E > 2.1$ keV) photon energy band, scaled between 0 and 8.5 counts per beam. Both of these Chandra images have been smoothed with a $2''$ beam. The cometary nebula is most apparent in the hard band image (right), while the soft point source stands out well against the surrounding nebula in the soft band image (left).

2.2. Very Large Array

All radio observations were made on August 26 and December 31, 1997 with the *Very Large Array* (VLA³) in the C and D arrays, respectively. A log of the observations is summarized in Table 1. The data acquisition and calibration were standard, using J0632+103 as a phase calibrator and 3C 138 as both the flux density and polarization angle calibrator.

The cometary and bow-shock morphologies of the extended source are even more pronounced at radio wavelengths, extending some $2'$ to the northeast of the soft X-ray source. Although we display only the $\lambda 3.5$ cm image in Figure 2, similar structure is visible at $\lambda 6$ cm and $\lambda 20$ cm. The peak in the radio emission lies about $6''$ to the northeast of the compact X-ray source. There is no radio point source (> 2 mJy) coincident with the X-ray point source. The distribution of linearly polarized emission is also shown in Figure 2. The direction of the E-vectors are generally parallel to the shock normal, as would be expected for evolved SNRs with circumferential magnetic fields. The character of the magnetic field evidently changes substantially in the area dominated by the X-ray emission. Here the magnetic field direction appears to wrap around the “head” of the hard nebula, tracing a bow-shock morphology. The average degree of polarization in this region is 8%. This is likely a lower limit since, owing to the compact size of the nebula, there is likely some beam depolarization occurring. To the northeast, where the field is more ordered, the percentage polarization is uncharacteristically strong for an evolved SNR, exceeding 25% in several locations.

³The VLA is operated by the National Radio Astronomy Observatory, a facility of the National Science Foundation.

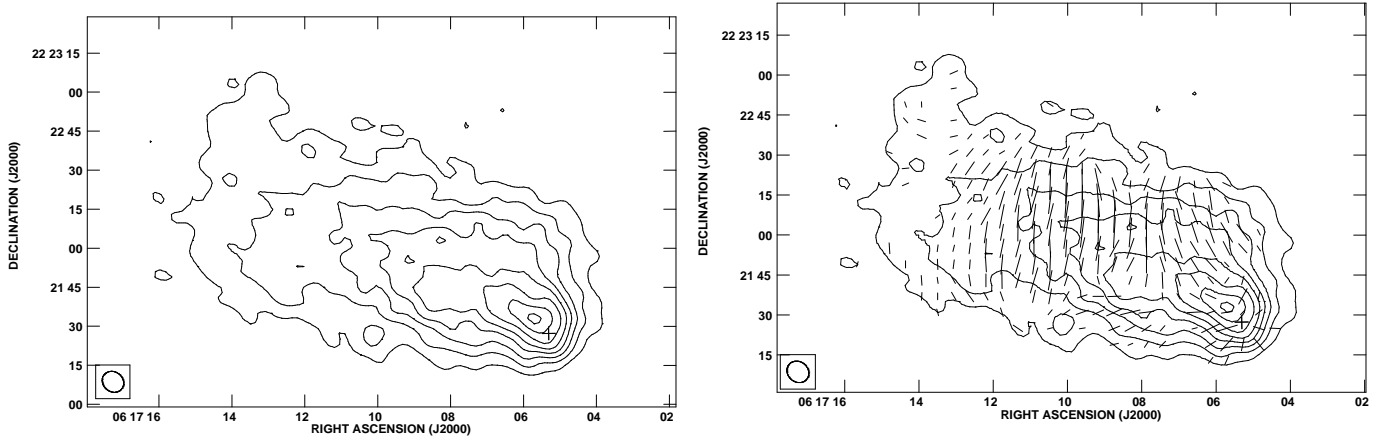


Fig. 2.— Total intensity image of the cometary nebula in IC 443 (left) at a frequency of 8.46 GHz. Contours are in steps of $0.5 \text{ mJy beam}^{-1}$. The size of the synthesized beam is shown in the lower left corner. The same total intensity image with vectors indicating the magnitude and direction of the polarized intensity (right). The scale is $50 \mu\text{Jy beam}^{-1} \text{ arcsec}^{-1}$. The cross marks the position of CXOU J061705.3+222127.

The integrated flux density over the entire length of the cometary nebula is given for three frequencies in Table 1. An approximate value of $230 \pm 200 \text{ mJy}$ was also obtained from the 327 MHz image presented by Claussen et al. (1997). The increased error in estimating the flux density at low frequencies is due to the uncertainty in subtracting out the background shell emission from the SNR. Within the errors, the radio spectrum is well represented by a flat spectral index $\alpha_R \simeq 0.0$ and a mean flux density of 206 mJy. In contrast, K97 measured an X-ray spectral index of $\alpha_X \simeq 1.3 \pm 0.2$, which implies a break in the spectrum near $4 \times 10^{13} \text{ Hz}$. The radio luminosity of the cometary nebula, determined by integrating the spectrum from 10 MHz to 100 GHz, is $L_R = 5.5 \times 10^{31} (d/1.5 \text{ kpc})^2 \text{ erg s}^{-1}$, or less than 1% of L_R for IC 443 as a whole.

Table 1. Summary of VLA Observations of the Cometary Nebula

Frequency (GHz)	Time (min)	Beam ($'' \times ''$)	F_ν (mJy)
8.46	13	8.6×7.6	195 ± 8
4.86	36	5.0×4.8	173 ± 11
1.46	53	15.5×14.5	229 ± 34

Note. — The columns are (left to right), (1) Observing frequency, (2) total time on source, (3) angular resolution, and (4) integrated flux density of the cometary nebula.

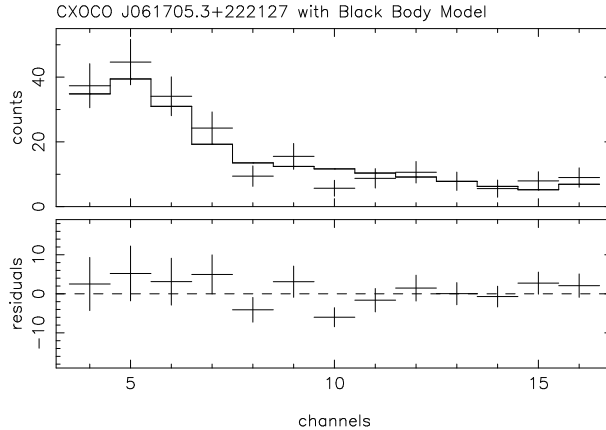


Fig. 3.— The background subtracted spectrum of the soft point source, fit with a black body emission model ($kT=0.7\pm 0.1$ keV and $A=0.02\pm 0.01(d/1.5\text{ kpc})^2\text{ km}^2$), assuming a previously measured column density. Channels 5, 10 and 15 correspond to photon energies of 1.5, 2.9, and 4.2 keV respectively.

2.3. Spectra

In addition to the spectral properties of the hard nebula, a spectrum of CXOU J061705.3+222127 was extracted from this short *Chandra* observation. The surrounding hard nebula was subtracted as background (i.e. an annulus with an inner and outer radius of $4.3''$ and $23.6''$ respectively). These spectra were binned by a factor of 256 (PHA channels), and the softest three ACIS-I channels were ignored. As discussed above, the point source is significantly softer than the surrounding hard nebula, implying a likely thermal origin for the emission. For this reason, we modeled the spectrum as black body radiation, though this fit was not statistically unique due to large uncertainties in the small data set.

The best-fit ($\chi^2_\nu \sim 1.1$) black body temperature and luminosity are $kT=0.71\pm 0.08$ keV and $L=(6.5\pm 0.9)\times 10^{31}\text{ erg s}^{-1}$ (i.e. $A=0.025\pm 0.003(d/1.5\text{ kpc})^2\text{ km}^2$). The 1-5 keV X-ray flux of the point source is $\sim 2\times 10^{-13}\text{ erg s}^{-1}\text{ cm}^{-2}$. This fits contained two free parameters by assuming K97’s best-fit column density ($N_H=1.3\times 10^{21}\text{ cm}^{-2}$).

3. Discussion

The soft X-ray point source in IC 443 is one of a growing number of young neutron star candidates associated with supernova remnants (Helfand 1998). These neutron stars have a diverse range of properties, suggesting that they do not originate from a homogeneous population (Chakrabarty *et al.* 2000). The long-period (8-10 s) and claimed high-field (10^{14} - 10^{15} G) of anomalous X-ray pulsars (AXP) and soft gamma-ray repeaters (SGR), differ from the canonical young radio pulsars with periods $P\sim 15$ -500 ms and field strengths of $B\sim 10^{12}$ - 10^{13} G. The radio quiet neutron stars (RQNs), with their thermal X-ray emission and lack of radio pulsations, may be altogether different from either of these two classes of objects (Pavlov *et al.* 2000).

In the absence of detectable pulsations, canonical radio pulsars can be distinguished from AXPs, SGRs, and RQNs by the presence of an extended synchrotron nebula, powered by the energetic relativistic wind (Gaensler, Bock & Stappers 2000). It is argued that the cometary nebula around the X-ray point

source in IC 443 is most likely such a PWN. This nebula has all the expected observational characteristics (C99; Gaensler *et al.* 2000): flat spectrum radio emission ($\alpha_R = 0.1$ to 0.3), a steep X-ray spectrum ($\alpha_X = 1.0$ to 1.5) and a high degree of linear polarization ($> 5\%$). Morphologically it closely resembles PWN detected toward the SNRs W 44 and G 5.4–1.2 (Frail & Kulkarni 1991; Frail *et al.* 1996), both of which contain active pulsars. It has been argued (Frail & Kulkarni 1991; Frail *et al.* 1996) that these nebulae have developed bow shocks as a result of ram pressure confinement of the pulsar wind, due to the high space velocity of their pulsar through the surrounding medium. We assert that the most tenable explanation for the X-ray point source in IC 443 is that it is a young pulsar which has traveled (ballistically) from its birth place to its present location, near the edge of the decelerating SNR.

Accepting this hypothesis we proceed with inferring the salient physical properties of the neutron star and corresponding PWN. Constraints can be placed on the velocity of the neutron star by a variety of methods. The offset of the object from its origin gives a measure of its transverse velocity V_{NS} . Measuring this offset in the case of IC 443 is made difficult owing to the uncertain location of the explosion center (Asaoka & Aschenbach 1994; Claussen *et al.* 1997). We note that the neutron star has traveled a fraction $\beta \simeq 0.9$ of this projected distance (approximated from the distance between the soft point source and the shock), giving $V_{NS} = \beta r_s / t_s$. Likewise, the shock velocity of the SNR can be similarly expressed as $V_s = c_o r_s / t_s$, where c_o is a constant equal to $2/5$ for a remnant in the Sedov stage, while C99 argues for a value of $c_o = 3/10$ for IC 443 based off of the parameters of his model. Combining both equations for V_{NS} and V_s together, and using the value of $V_s = 100 \text{ km s}^{-1}$ favored by C99, gives $V_{NS} = V_s \beta c_o^{-1} = 225\text{-}300 \text{ km s}^{-1}$, a result that is independent of distance and only weakly dependent on the evolutionary state of the SNR (i.e. c_o).

It should be noted that the tail of the hard nebula does not point towards the geometric center of the SNR. However, the blast center and geometric center of an SNR can be quite different in the presence of large-scale density gradients (Dohm-Palmer & Jones 1996; Hnatyk & Petruk 1999). Such a density gradient, combined with the potential of a cross-wind, could possibly account for the apparent discrepancy.

We are able to make a second approximation of V_{NS} with respect to the local medium by means of the nebula’s bow shock morphology. K97 fit the SNR with an X-ray temperature $kT \simeq 1 \text{ keV}$, implying a sound speed $c_{local} \simeq 100 \text{ km s}^{-1}$. An approximation of the bow shock angle of $90^\circ\text{-}120^\circ$ gives a minimum Mach number $M \simeq 1.1\text{-}1.5$ through a standard geometric calculation. A fundamental determination of the speed of sound in this particular region of the SNR gives velocity with respect to the local medium of $V_{NS\ local} = 150 M_{1.5} kT_{1\ keV}^{0.5} \text{ km s}^{-1}$. Accounting for radial expansion of local plasma ($\leq 100 \text{ km s}^{-1}$, this velocity could be as high as 250 km s^{-1}). Both methods of determining V_{NS} are in good agreement with a model by C99, indicating a remnant age on the order of 30,000 years (i.e. $\tau_{30} \simeq 1$).

The energy source for the synchrotron nebula must ultimately be derived from the particles and field generated by the compact central neutron star and therefore some fraction of the its spindown power \dot{E} is powering this emission. Empirical relations have been derived for known PWN between \dot{E} and the observed X-ray and radio luminosities (L_x and L_R) that enable us to estimate the rotation period P and the magnetic field B of the compact object.

For the value of L_x derived in §2 we obtain $\dot{E} \sim 2 \times 10^{36} \text{ erg s}^{-1}$ (Seward and Wang 1988). Frail & Scharringhausen (1997) and Gaensler *et al.* (2000) note that $\dot{E} \sim 10^4 L_R$ for known radio PWN, which yields a value of $\dot{E} \sim 6 \times 10^{35}$, so in the discussion that follows we adopt $\dot{E} = 10^{36} \text{ erg s}^{-1}$ (i.e. $\dot{E}_{36} = 1$). Equating the pressure of the wind $\dot{E}/4\pi cr_w^2$, to the ram pressure due to the neutron star’s motion through the surrounding gas ρV_{NS}^2 , we derive a density of $\sim 0.1 \text{ cm}^{-3}$ for our adopted values of \dot{E} and V_{NS} . This

density is more typical of that expected for the hot X-ray interior of the SNR, and is orders of magnitude below that expected in the dense molecular ring against which the NS and its nebula are projected against (see van Dishoeck et al. 1993).

The spindown luminosity of a pulsar is related to its current period P and dipolar surface field B by $\dot{E} \propto B^2 P^{-4}$, while the characteristic age of the pulsar is expressed as $\tau_c \propto B^{-2} P^2$. It is straightforward to show that for a pulsar born spinning rapidly (i.e. $P_o \ll P$), which loses energy predominately via magnetic dipole radiation, $P=145 \text{ ms } (\tau_{30} \dot{E}_{36})^{-1/2}$ and $B=3.3 \times 10^{12} \text{ G } \tau_{30}^{-1} \dot{E}_{36}^{-1/2}$. Thus, with our nominal choice of parameters, the period and magnetic field closely match those of other young pulsars (e.g. PSR B1757–24; Frail & Kulkarni 1991).

In the light of this result, it is worth re-examining the nature of the unidentified EGRET source 2EG J0618+2234 (l,b=189.13°, +3.19°) (Sturmer & Dermer 1995; Esposito *et al.* 1996) toward IC 443. Nel et al. (1996) note that all known gamma-ray pulsars have a large (greater than 0.5) ratio of \dot{E}_{33}/d_{kpc}^2 . For our derived $\dot{E} \sim 10^{36} \text{ erg s}^{-1}$ and $d \sim 1.5 \text{ kpc}$, this ratio is over 400, similar to that of the gamma-ray emitting PSR B1706–44, strongly suggesting that the unidentified EGRET emission originates from the neutron star or the PWN. The difficulty with this interpretation is that our proposed neutron star and PWN lie several arcminutes outside the formal 95% error radius of the EGRET source. However, since the position of EGRET sources in the Galactic plane are subject to systematic error (e.g. Hunter *et al.* 1997), it is entirely possible that this object may be the source of this gamma-ray emission.

4. Conclusion

In summary, the hard X-ray feature in IC 443 is best interpreted as a wind nebula powered by a young neutron star. The PWN interpretation is suggested first on morphological grounds by the Chandra and VLA images, which show a comet-shaped nebula with a soft X-ray point source at its apex. The measurement of significant polarization and a flat radio spectrum further strengthens the argument that this is synchrotron emission from a PWN. The X-ray spectrum of the point source is appropriately, but not uniquely fit by a black body model, suggesting that the emission is thermal in origin. The inferred physical properties of the nebula and point source (i.e. τ , V_{NS} , \dot{E} , P , B) support our hypothesis that IC 443 and the pulsar were produced approximately 30,000 years ago in a core collapse supernova event.

Despite the evidence in favor of a real physical association between IC 443 and the compact source within the cometary nebula, there are a few puzzles that remain to be explained. As mentioned previously, one might expect the “tail” of the cometary nebula to point back to the origin of the SNR and the pulsar. However, the geometric center of IC 443 lies almost due north of the compact object, and not to the northeast as suggested by the direction of the cometary tail. Given the complex kinematics and distribution of the molecular and neutral gas in the vicinity of IC 443 (Giovanelli & Haynes 1979; van Dishoeck *et al.* 1993) it may be overly naïve to ascribe the blast center to the geometric center. A final problem concerns the apparent absence of X-ray and radio pulsations from the IC 443 point source. K97 carried out a pulse search using *ROSAT* and *ASCA* data, while Kaspi et al. (1996) have searched for radio pulsations. In our view, these null results present no immediate problem for our young neutron star hypothesis since pulsed X-rays from Vela-like pulsars have proven difficult to detect due to their soft spectra and contamination from the surrounding nebular emission (e.g. Becker & Truemper 1997). Furthermore, it is entirely possible that the radio beam may not intersect our line of sight (Lorimer, Lyne & Camilo 1998).

We thank D. J. Thompson, B. M. Gaensler, R. Petre, P. Slane, R. A. Chevalier, R.A. Fesen, and J. Kolena for useful discussions, and referee Randall Smith for his thoughtful comments. We also thank G. E. Allen, K. A. Arnaud, J-H. Rho, N. Evans, and M. Johnson for help with data analysis. This research was funded by NASA grant NRA 97-OSS-14.

REFERENCES

- Asaoka, I. and Aschenbach, B. 1994, *A&A*, 284, 573.
- Baring, M. G., Ellison, D. C., Reynolds, S. P., Grenier, I. A., and Goret, P. 1999, *ApJ*, 513, 311.
- Becker, W. and Truemper, J. 1997, *A&A*, 326, 682.
- Bocchino, F. & Bykov, A. M. 2000, *A&A*, 362, L29
- Braun, R. and Strom, R. G. 1986, *A&A*, 164, 193.
- Burton, M. G., Hollenbach, D. J., Haas, M. R., and Erickson, E. F. 1990, *ApJ*, 355, 197.
- Bykov, A. M., Chevalier, R. A., Ellison, D. C., and Uvarov, Y. A. 2000, *ApJ*, 538, 203.
- Chakrabarty, D., Pivovarov, M. J., Hernquist, L. E., Heyl, J. S., and Narayan, R. 2000, *apj*. in press (astro-ph/0001026).
- Chevalier, R. A. 1999, *ApJ*, 511, 798.
- Claussen, M. J., Frail, D. A., Goss, W. M., and Gaume, R. A. 1997, *ApJ*, 489, 143.
- Dohm-Palmer, R. C. and Jones, T. W., 1996, *ApJ*, 471, 279
- Esposito, J. A., Hunter, S. D., Kanbach, G., and Sreekumar, P. 1996, *ApJ*, 461, 820.
- Fesen, R. A. 1984, *ApJ*, 281, 658.
- Frail, D. A., Giacani, E. B., Goss, W. M., and Dubner, G. 1996, *ApJ*, 464, L165.
- Frail, D. A. and Kulkarni, S. R. 1991, *Nature*, 352, 785.
- Frail, D. A. and Scharringhausen, B. R. 1997, *ApJ*, 480, 364.
- Gaensler, B. M., Bock, D. C. ., and Stappers, B. W. 2000, *ApJ*, 537, L35.
- Gaensler, B. M., Stappers, B. W., Frail, D. A., Moffett, D. A., Johnston, S., and Chatterjee, S. 2000, *mnras*, 318, 58.
- Gaisser, T. K., Protheroe, R. J., and Stanev, T. 1998, *ApJ*, 492, 219.
- Giovanelli, R. and Haynes, M. P. 1979, *ApJ*, 230, 404.
- Green, D. A. 1986, *MNRAS*, 221, 473.
- Helfand, D. J. 1998, *Memorie della Societa Astronomica Italiana*, 69, 791.
- Hnatyk, B. and Petruk, O. 1999, *A&A*, 344, 295

- Hunter, S. D. *et al.* 1997, *ApJ*, 481, 205.
- Keohane, J. W., Petre, R., Gotthelf, E. V., Ozaki, M., and Koyama, K. 1997, *ApJ*, 484, 350.
- Kovalenko, A. V., Pynzar, A. V., and Udal'Tsov, V. A. 1994, *Astronomy Reports*, 38, 95.
- Lorimer, D. R., Lyne, A. G., and Camilo, F. 1998, *A&A*, 331, 1002.
- Nel, H. I. *et al.* 1996, *A&AS*, 120, C89.
- Pavlov, G. G., Zavlin, V. E., Aschenbach, B., Trümper, J., and Sanwal, D. 2000, *ApJ*, 531, L53.
- Petre, R., Szymkowiak, A. E., Seward, F. D., and Willingale, R. 1988, *ApJ*, 335, 215.
- Seward, F. D. and Wang, Z. 1988, *ApJ*, 332, 199.
- Sturmer, S. J. and Dermer, C. D. 1995, *A&A*, 293, L17.
- Sturmer, S. J., Dermer, C. D., and Mattox, J. R. 1996, *A&AS*, 120, C445.
- Sturmer, S. J., Skibo, J. G., Dermer, C. D., and Mattox, J. R. 1997, *ApJ*, 490, 619.
- van Dishoeck, E. F., Jansen, D. J., and Phillips, T. G. 1993, *A&A*, 279, 541.
- Wang, Z. R., Asaoka, I., Hayakawa, S., and Koyama, K. 1992, *PASJ*, 44, 303.

CXOC0 J061705.3+222127 with Power Law Model

